DOI: 10.3901/CJME.2012.02.223, available online at www.springerlink.com; www.cjmenet.com; www.cjmenet.com.cn

Development of a Hand Exoskeleton System for Index Finger Rehabilitation

LI Jiting*, WANG Shuang, WANG Ju, ZHENG Ruoyin, ZHANG Yuru, and CHEN Zhongyuan

State Key Laboratory of Virtual Reality Technology and Systems, Beihang University, Beijing 100191, China

Received September 8, 2010; revised April 27, 2011; accepted April 30, 2011

Abstract: In order to overcome the drawbacks of traditional rehabilitation method, the robot-aided rehabilitation has been widely investigated for the recent years. And the hand rehabilitation robot, as one of the hot research fields, remains many challenging issues to be investigated. This paper presents a new hand exoskeleton system with some novel characteristics. Firstly, both active and passive rehabilitative motions are realized. Secondly, the device is elaborately designed and brings advantages in many aspects. For example, joint motion is accomplished by a parallelogram mechanism and high level motion control is therefore made very simple without the need of complicated kinematics. The adjustable joint limit design ensures that the actual joint angles don't exceed the joint range of motion (ROM) and thus the patient safety is guaranteed. This design can fit to the different patients with different joint ROM as well as to the dynamically changing ROM for individual patient. The device can also accommodate to some extent variety of hand sizes. Thirdly, the proposed control strategy simultaneously realizes the position control and force control with the motor driver which only works in force control mode. Meanwhile, the system resistance compensation is preliminary realized and the resisting force is effectively reduced. Some experiments were conducted to verify the proposed system. Experimentally collected data show that the achieved ROM is close to that of a healthy hand and the range of phalange length (ROPL) covers the size of a typical hand, satisfying the size need of regular hand rehabilitation. In order to evaluate the performance when it works as a haptic device in active mode, the equivalent moment of inertia (MOI) of the device was calculated. The results prove that the device has low inertia which is critical in order to obtain good backdrivability. The experiments also show that in the active mode the virtual interactive force is successfully feedback to the finger and the resistance is reduced by one-third; for the passive control mode, the desired trajectory is realized satisfactorily.

Key words: exoskeleton, hand rehabilitation, Bowden-cable transmission, active control mode, passive control mode

1 Introduction

Hand is one of the most important organs of human body, and its function is crucial for people's daily living activities. However, accident and diseases, stoke for instance, can lead to loss of sensation and motor functions of hand. In order to recover the lost functions, hand rehabilitative trainings are needed[1], which basically consists of passive and active rehabilitative motion from the perspective of patient. Traditional rehabilitation has some drawbacks which need to be overcome with the aid of new engineering techniques. Firstly, rehabilitation need long term exercises for patients which might last for several months to even years. Secondly, the rehabilitative exercises are tedious and boring that could not arouse strong desire and motivation to patients. These two factors make it very difficult for the patients to insist on doing the rehabilitation exercises. Thirdly, rehabilitation procedure needs therapists to instruct or even to aid the patients doing exercises directly, so very large quantities of therapists are needed. However, the present number of therapists cannot satisfy the requirement and the lack of therapists results in the rehabilitative therapy very expensive. Additionally, therapy and evaluation depend on the experience of therapist which causes less objectivity of the assessment of rehabilitation.

Recent researches showed that the method of incorporating mechatronic devices and the technology of virtual reality into hand rehabilitative training is feasible and effective[2–3]. Besides excelling at repetitive controlled movement, and these devices have the potential to assess the rehabilitation objectively by integrating with necessary sensors[4]. However, for the developed hand rehabilitation devices, the realizable exercises are different. Some aimed at finger's simple actions such as pinch, or closing and opening[5]. This kind of rehabilitation device usually has simple structure but with less DOFs. Some others devote to providing broader exercises, especially training the finger's

* Corresponding author. E-mail: lijiting@buaa.edu.cn
This project is supported by National Natural Science Foundation of China (Grant No. 50975009)

manipulation ability. We only emphasize the latter kind of investigation thereafter. In terms of the way by which they interface with human hand, we roughly classify the hand rehabilitation devices into two categories, which we respectively name on-fingertip device and hand exoskeleton. For the on-fingertip devices, the thimble which is attached on the user's fingertip is usually the only interface between the finger and the device. The device cannot get the information of each finger joint independently nor apply torques to joints directly. One of the representative examples is HIFE[6] developed at the *University of Ljubljana of Slovenia*. It has two active degrees of freedom for finger exercises. The cooperated researchers at the *National University of Singapore*, *Imperial College London of UK*, and *Simon Fraser University of Canada* developed a cable driven underactuated robotic system which is driven by only one actuator and a clutch system and can train the fingers with selected tasks [7].

Hand exoskeleton is more widely investigated though it is more complicated than the on-fingertip type. Some of them are developed as the force feedback devices[8–10], which can only apply force in single direction and cannot drive the finger bi-directionally, so they can only be used in active rehabilitative mode. Such instances are the devices designed at the *Gifu University of Japan*[11] which works under the self-motion control mode and each finger has three DOFs. *Harbin Institute of Technology of China*[12] developed an exoskeleton with four DOFs which can realize the passive rehabilitative training. The exoskeleton developed by WEGE, et al, at the *Technical University of Berlin of Germany*[13] has 4 DOFs and can actuate each finger joint by the means of linkage mechanism, but the additional changeable attachments are needed to fit for the different hand sizes. WORSNOPP, et al, at *Northwestern University of the United State*[14] proposed a virtual prototype with 3 DOFs which can only be assembled on the lateral side of the finger, so it cannot be applied to the middle and ring fingers. YAMAURA, et al, at *University of Tokyo of Japan*[15] proposed a hand rehabilitation device that can be adjustable to accommodate various hand sizes but only has two DOFs for each finger. HANDEXOS which is developed by CHIRI, et al[16], at *ARTS Lab Scuola Superiore Sant'Anna* of Italy has three active rotational joints for flexion/extension, one passive rotational joint for abduction/adduction, and one passive translational joint for kinematic coupling of the human/exoskeleton MP axes for each finger.

Despite of the wide researches, due to the special application of human hand rehabilitation, there are many unsolved issues suspending and design of exoskeletons is still an investigation field full of challenges.

This paper investigates the design of a hand exoskeleton for motor capability rehabilitation that simultaneously fulfills the following requirements: (1) Work in both passive and active rehabilitative training modes; (2) Control all of finger joint independently; (3) Fit for the evolving feature of rehabilitation, which means the joint ROM is changable during the rehabilitation process; (4) Suit for different hand sizes; (5) Comply with human hand anatomy and don't interfere with fingers. In addition, lightweight and safety issues must be taken into account as well. To satisfy the above mentioned requirements, we adopted the scheme which decoupled the actuators far from the hand by Bowden cable transmission similar with Refs. [12] and [13], and proposed the parallelogram mechanism to be the exoskeleton mounted on the dorsal side of the hand to drive or follow with the human fingers. With this schematic structure, the new device can actuate and control each finger joint independently and bi-directionally, which provides the fundamental to realize both passive and active rehabilitation modes. With the special mechanical design, the other requirements are satisfied as well, which are described in the following sections. One of the especial advantages is that the joint angle relationship between the device and the corresponding human finger is very simple which makes the high level control very convenient.

The rest parts of this paper are arranged as follows. We commence with the system description in section 2. We subsequently present the mechanical design and some specification analysis of the device in section 3. Then the control method is described in section 4. The conclusion of our investigation and future work are discussed in the last section.

2 System Description

The proposed architecture of hand rehabilitation system is shown in Fig. 1, which consists of the hand exoskeleton, the control (including controller and driver), and the virtual environment.

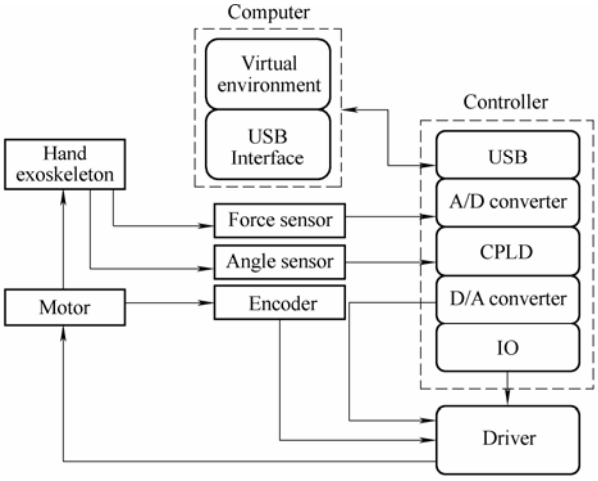

Fig. 1. Proposed architecture of hand rehabilitation system

The exoskeleton of the device (excluding the actuation

and transmission parts) is put on the human hand and integrated with angle and force sensors to measure the joint angles and the force exerted by the hand. It can be driven by or can drive human hand according to different rehabilitation modes.

The controller is developed by our research group, as shown in Fig. 2. It can sample the angle and force data in real time. The controller links to the host computer by the USB port, and the sampling frequency is 100 Hz. The motor driver (EM-28 DC-MOTOR CONTROL UNIT, Finland) is connected to the controller through analog output channels, and runs under the torque control mode.

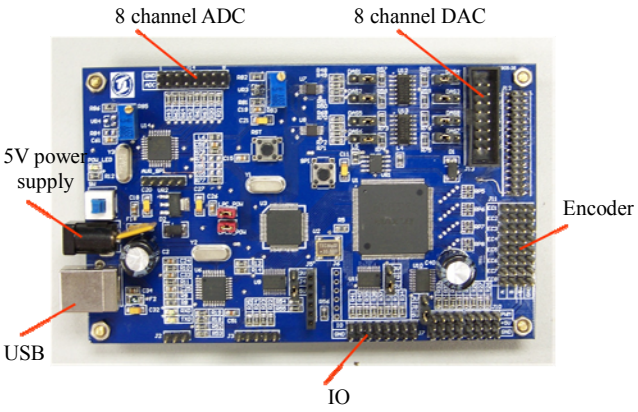

Fig. 2. Layout of controller

The host computer runs the virtual rehabilitation environment and gives the virtual interactive force feedback to the patient in active rehabilitative motion. The operation interface provides to calibrate the exoskeleton, choose the rehabilitation mode, and set the training parameters, for example, ROM, training time, training speed and so on. In the graphic interface, the virtual hand, which is controlled by the human hand, is used to accomplish the different virtual rehabilitation tasks.

3 Design and Analysis of the Exoskeleton Device

Because the four fingers have the same anatomical structure except that the phalange lengths of different digits are different, from the perspective of kinematics the proposed exoskeleton scheme is suitable for all the four fingers and therefore the following description only takes the index finger for example.

As illustrated in Fig. 3, the exoskeleton device consists of three parts: the actuation module, the Bowden cable transmission, and the exoskeleton mounted on the dorsal side of the hand. The detailed design is described in the following subsections.

3.1 Model of index finger

Compliance with the human hand anatomy is the premise for the designed exoskeleton able to be worn on the human hand. The anatomical structure of index finger is comprised of three phalanges—distal, middle and proximal phalanges, which are connected in sequence by distal interphalangeal (DIP) joint, proximal interphalangeal (PIP) joint and metacarpaophalangeal (MCP) joint to metacarpal. The joint structures are complicated and difficult to completely copy in mechanical design. So the finger's kinematic structure should be reasonably simplified. As shown in Fig. 4, the index finger is modeled as a serial four-bar linkage with four DOFs. The DIP and PIP joints are modeled as one-DOF hinges to realize the flexion/extension motions, while the MCP joints is simplified as two one-DOF hinges (denoted by MCP 1 and MCP2, respectively) with orthogonal and intercrossing rotating axis to realize the corresponding motions of flexion/extension and adduction/abduction. And the anthropometric data, including the average length of finger phalanges, ROM of finger joints, and the maximum joint torque which can be applied to finger joints[1, 17, 18] are listed in Table 1. These data are the design parameters of exoskeleton device and can be used to evaluate our design later.

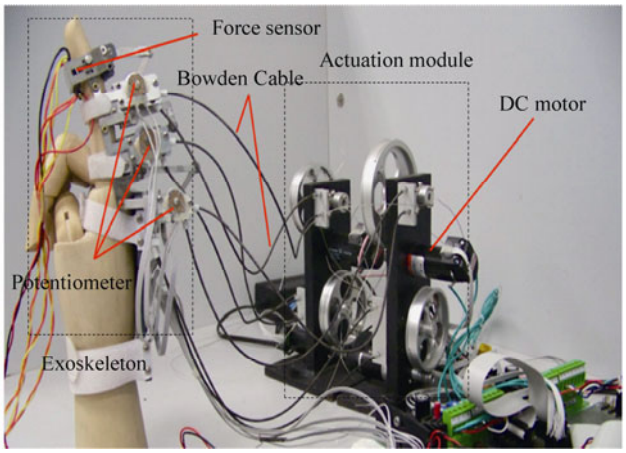

Fig. 3. Aactuation, transmission and hand exoskeleton

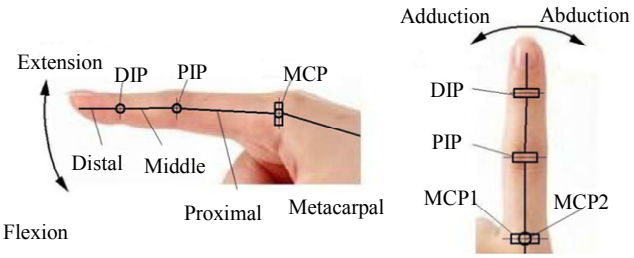

Fig. 4. Kinematic model of index finger

3.2 Design of the hand exoskeleton

In order to cover the range of finger motion listed in Table I and prevent interference with other fingers, the exoskeleton is mounted on the dorsal side of hand and be fixed by Velcro, as shown in Fig. 3. The mechanical structure is demonstrated in Fig. 5. Corresponding to the

aforementioned index finger model, it consists of three joint modules: DIP, PIP, and MCP modules, which respectively realize the motion of DIP, PIP, MCP1, and MCP2 joints of the index finger. So the exoskeleton can realize all 4 DOFs of an index finger.

Table 1. Anthropometric data of index finger

Joint	DIP	PIP	MCP1	MCP2
ROM θ/(°)	0–80	0–100	0–85	0–45
Max-torque τ/(N • m)	0.17	0.29	0.29	0.20
Phalange	Distal	Middle		Proximal
Length l/mm	17	25		43

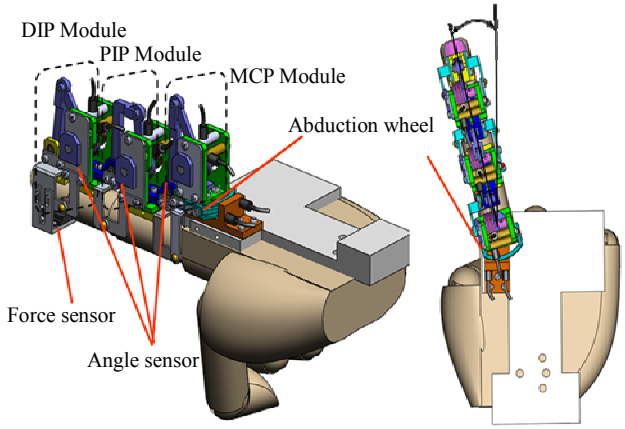

(a) Joint modules　　(b) Abduction

Fig. 5. Virtual Prototype

Considering that the simple relationship between the joint angles of exoskeleton and that of human finger will bring great convenience to high level motion control of the device as well as to measure the joint angles of human hand, the parallelogram mechanism is adopted. We take the DIP joint module for instance to describe the design in more detail. As shown in Fig. 6, links 7−10 constructs the parallelogram mechanism in which link 7 is fastened to the middle phalange and thus is the relative fixed link; link 8 is the driving link which is driven by the Bowden cable transmission; and link 10 is fastened to the distal phalange of the finger. The rotating angle of link 10, $\Delta\theta$, which is also the rotating angle of finger's DIP joint, is always equal to that of the link 8, $\Delta\alpha$, which can be directly measured by the angle sensor (as shown in Fig. 5 (a)) installed on the shaft of link 8. Therefore if the angle of finger joint is given to be controlled, it can be easily realized by controlling the link 8 to rotate the same angle. The links are designed according to the finger phalangeal lengths and the allowed space to avoid the collision with the parts of the adjacent joint modules. The PIP and MCP1 joint modules are also constructed with the same method.

The motion of MCP2 joint, which is the abduction/adduction motion of finger, is realized by directly driving the abduction wheel which is beneath the MCP1 joint module, as shown in Fig. 5.

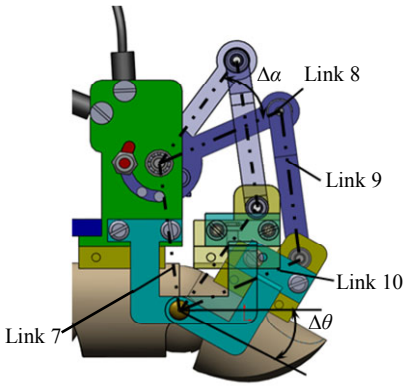

Fig. 6. Parallelogram mechanism for DIP joint

All joints are supported with ball bearings and the material of most parts is aluminum. The mass of the hand exoskeleton is 160 grams. To our knowledge the weight is acceptable to human hand.

Accommodation to different sizes of human hand is also accomplished. As we know, the different hand size generally implies that the lengths of finger phalanges are different. The phalange lengths is respectively referred to as the distance from fingertip to DIP joint, the distance from DIP to PIP joints, and the distance from DIP to MCP1 joints. When the exoskeleton is put on the human hand, the joints J_{DIP}, J_{PIP} and J_{MCP1} of the exoskeleton need to be aligned with those of the finger joints, respectively, which means that the distance l'_M and l'_P are required to be changeable to accommodate different sizes of hand, as shown in Fig. 7. In our design, the relative positions of adjacent joint modules are adjustable with two screws. By fastening the screws at different positions along the slots, the changed lengths are accomplished.

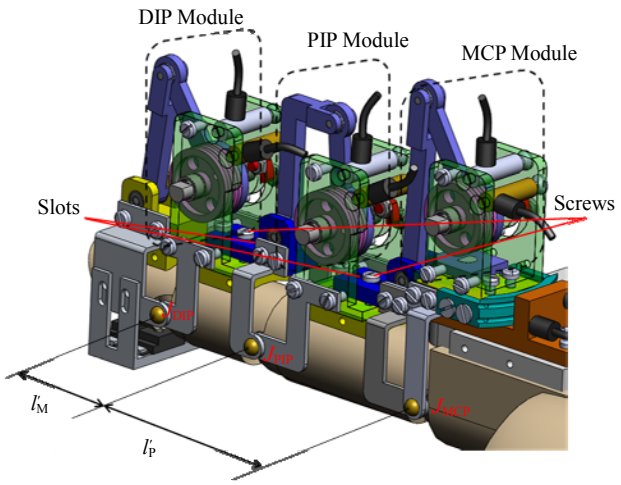

Fig. 7. Adjustment of positions of joint modules

The adjustable range of length is 22 mm−30 mm for middle phalange, and 40 mm−50 mm for proximal phalange, as demonstrated in Fig. 8. There is no constraint to the length of distal phalange. Compared with the data in Table I, the result is shown in Table 2. It is obviously that

the exoskeleton covers the average hand size completely and suits to the somewhat ranges of hand size.

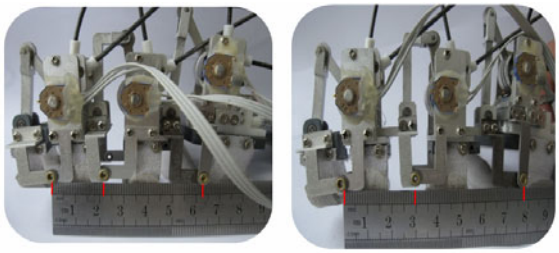

Fig. 8. Range of phalange length

Table 2. Comparison of the Length of Phalange

Phalange	Middle	Proximal
Mean Length l/mm	25	43
Adaptable range of length l/mm	22–30	40–50

Safety issue is another important concern. Especially for the impaired hand, because of the loss of sensation and motor ability, the patient hand is much more vulnerable. Safety design in mechanical structure, combined with the safety guarantee in software and control, provides the patient hand multiple protections from being re-hurt. Different patients have different motor capabilities and even if for one patient the ROM can gradually change during the process of rehabilitative training. So the maximum rotational angle needs to be able to be limited at various positions. A mechanical structure is designed to meet the requirement. Take the DIP module for instance, as illustrated in Fig. 9. The stop slider can slide along an arc slot which is coaxial with the rotation axis of the driving link. And a stop pin fixed on and rotating together with the driving link can also move along the arc slot. The maximal angle between the stop pin and stop slider determines the allowed ROM. By fixing the stop slider at different position along the arc slot, the ROM can be modified. So this structure can adapt different patients with different motor abilities by the means of providing the changeable ROM.

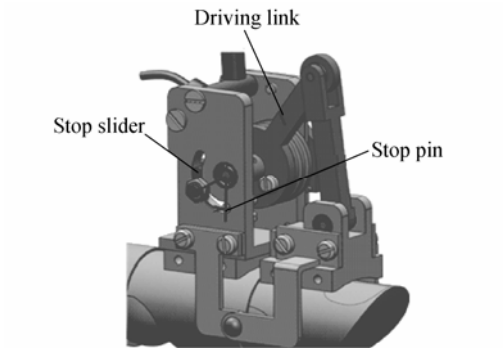

Fig. 9. Mechanical stop structure of joints

3.3 Actuation and sensing systems

The actuation module is located distantly from the hand in order to reduce the weight imposed on the patient hand, as shown in Fig. 2. Four motors are fixed on the desktop frame to provide force and motion which is transmitted to the four finger joints by a reducer and Bowden cable transmission. The detail description can be found in[19].

Angle sensors as well as force sensors are integrated in the exoskeleton. Four potentiometers (Murata SV01A103) are installed on the shafts of DIP, PID, MCP1, and MCP2 joint modules to measure the respective joint angles, as presented aforementioned.

Force sensors (Honeywell_FSS) are used to measure the fingertip force exerted by the human fingertips. Because the measure area (a small spherical surface) of the sensor is too small for soft fingertip to measure the reliable force, three sensors (shown in Fig. 10) are assembled together on the bottom of the distal module as shown in Fig. 10(a) and are covered with a thin metal plate as shown in Fig. 10(b). This ensures that the force exerted by the hand could be measured accurately. The forces on three contact points output from the three sensors are summed to obtain the resultant force which is exerted by the finger[20].

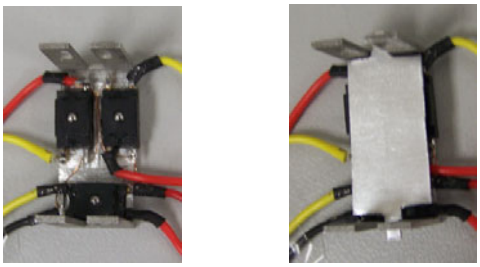

(a) Layout of three sensors (b) Covered by a metal plate

Fig. 10. Assembly of force sensors

3.4 Specification and equivalent MOI analysis of the device

Many requirements need to be satisfied for a hand rehabilitation device, thus evaluation of the device can be done from various perspectives and a comprehensive evaluation is difficult. We only evaluate the performances of our device from two aspects which we think they are very fundamental from the point of utility. The first one is range of motion (ROM) which affects the adaptability of the device to the patients and the second is the equivalent moment of inertial (MOI) which can represents the backdrivability of the device when the device is used in the active rehabilitation mode.

3.4.1 Range of motion

In order to get an effective rehabilitation effect, the ROM that exoskeleton allows the finger to reach should be approximate to the natural ROM of a healthy finger. To assess this performance, the maximal joint angles are measured when hand does not wear and wears the exoskeleton and the differences are compared. Ten healthy volunteers (5 females and 5 males) participated in the experiment. The experimental result is shown in Fig. 11. The black lines represent the range of the maximal joint angles of ten subjects for DIP, PIP, and MCP1 joints. The color columns are the corresponding average ROM. For

each pair the left and right column stands for the data without and with the exoskeleton respectively. The results show that the maximal angles of each joint with the device are somewhat various for different individuals, ranging from 65.6° −80.2° for DIP joint, 96.3° −119.7° for PIP joint, and 76.6° −92.0° for MCP1 joint which are smaller than those without exoskeleton. This is because the Velcro straps tightened the soft tissues of the volar side of the phalanges and thus constrained the motion of joints to some extent and the PIP joint is influenced the most. The average difference is 5.7° for DIP joint, 17.1° for PIP joints, and 6.6° for MCP1 joint, respectively. The exoskeleton has no restraint to the MCP2 joint. The result is acceptable considering that the patients have less motor ability than the healthy people and the slightly smaller limit angles is also a protection the patient.

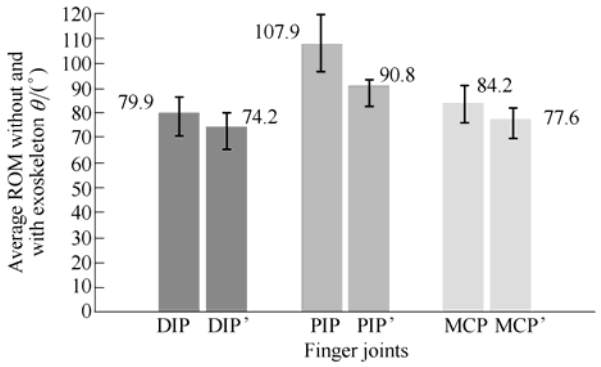

Fig. 11. ROM with and without exoskeleton

3.4.2 *Equivalent of moment of inertia*

Although there are four DOFs in the device, the DIP, PIP and MCP1 modules always flex and extend in the same plane. In addition, rehabilitation trainings are usually more focused on flexion/extension than abduction/adduction, the DOF of MCP2 is not taken into account here. So the mechanism of the exoskeleton can be treated as a planar mechanism with three DOFs and only the motions in this plane is analyzed in the following. Fig. 12 represents the schematic diagram of the planar mechanism. And the coordinate systems are set up in different modules according to the D-H method.

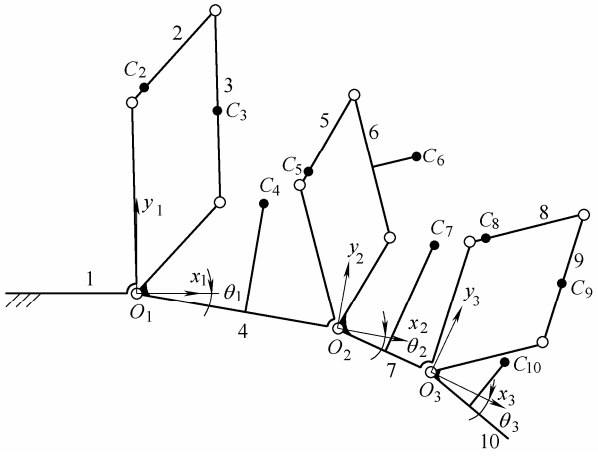

Fig. 12. Kinematic sketch of the hand exoskeleton

The moment of inertia (MOI) has a significant impact on the performance of the system, especially on backdrivability when the device is used in the active rehabilitation mode in which case it plays the same role as the haptic device and small inertial is admired. In rehabilitation application, the MOI effect, which is caused by the exoskeleton and actuation module, is felt by finger when it moves actively. Therefore we use the equivalent MOI seen from the different phalanges to measure this effect. And the links10, 7, 4, which are fixed with finger phalanges, are chosen to be the equivalent links. For every joint module, the equivalent MOI can be expressed as follows:

$$(J_{\mathrm{Ee}})_K = (J_{\mathrm{Ee}})_K + (J_{\mathrm{Ea}})_K , \tag{1}$$

where K can be DIP, PIP, and MCP1. J_{Ee} and J_{Ea} represent the equivalent MOI as seen from each joint caused by the exoskeleton and the actuation system, repectively.

(1) DIP joint module

We calculate the equivalent MOI of DIP joint module relative to the middle phalange which means link 7 is the relative fixed frame. As aforementioned with link 10 being regarded as the equivalent link, the equivalent MOI of the DIP module as seen from the DIP joint is obtained as follows according to the principle of equivalency of kinetic energy:

$$(J_{\mathrm{Ee}})_{\mathrm{DIP}} = \sum_{j=8}^{10}\left[m_j \left(\frac{{}^3v_{Cj}}{\omega_{10}} \right)^2 + J_j \left(\frac{\omega_j}{\omega_{10}} \right)^2 \right], \tag{2}$$

where ${}^3v_{Cj}$ is the linear velocity of the center of mass of the jth link relative to the coordinate system O_3-x_3y_3. And ω_j represents angular velocity of the jth link.

The equivalent MOI of the actuation module can be calculated with the same method:

$$(J_{\mathrm{Ea}})_{\mathrm{DIP}} = (J_{\mathrm{D}})_{\mathrm{DIP}} + (J_{\mathrm{T}})_{\mathrm{DIP}} + (J_{\mathrm{M}} + J_{\mathrm{S}})i_{\mathrm{DIP}}^2 , \tag{3}$$

where J_{M} and J_{S} denote the MOI of the motor and spiral wheel, respectively. J_{D} and J_{T} represent MOI of the driving wheel and transmission wheel, respectively. And i is the transmission ratio from motor shaft to driving link in hand exoskeleton.

From Eqs. (1)−(3), $(J_{\mathrm{E}})_{\mathrm{DIP}} = 5.34 \times 10^4$ g • mm^2.

(2) PIP joint module

As for the PIP joint, the DIP joint module becomes the end-effector, so it will bring additional MOI to PIP joint module. We calculate the equivalent MOI of PIP joint module relative to the proximal phalange and take link 4 as the relative fixed frame. Meanwhile, link 7 is treated as the equivalent link. Similar with the DIP joint, the equivalent MOI of the exoskeleton as seen from the PIP joint is calculated with the following equation:

$$(J_{\mathrm{Ee}})_{\mathrm{PIP}}=\sum_{j=5}^{10}\left[m_j\left(\frac{{}^{2}v_{Cj}}{\dot{\alpha}_2}\right)^2+J_j\left(\frac{\omega_j}{\dot{\alpha}_2}\right)^2\right]. \tag{4}$$

The variables denote the similar meaning in Eq. (2) and are not explained in detail again here.

Though PIP joint and DIP joint are designed to be able to move independently, when the human moves the finger freely, the rotating angle of DIP joint is coupled with that of PIP joint with the following relationship[21]:

$$\theta_3=\frac{2}{3}\theta_2 .$$

So their angular velocity relationship is obtained as follows:

$$\omega_{10}=\frac{2}{3}\omega_7 . \tag{5}$$

From Eqs. (4) and (5) it is easy to know that $(J_{\mathrm{Ee}})_{\mathrm{PIP}}$ is the function of the rotating angle of link 7, namely θ_2.

The equivalent MOI of the actuation module for the PIP joint is equal to that for the DIP joint because the actuation modules are same. So we have

$$(J_{\mathrm{Ea}})_{\mathrm{PIP}}=(J_{\mathrm{Ea}})_{\mathrm{DIP}} . \tag{6}$$

According to Eqs. (1) and (4)–(6), the maximal equivalent MOI for the PIP joint can be calculated:

$$(J_{\mathrm{E}})_{\mathrm{PIPmax}}=9.58\times10^4\ \mathrm{g\cdot mm^2}.$$

(3) MCP1 joint module

As for the MCP1 joint, the DIP and PIP joint modules are both the load, so their MOI should be included as well when we calculate the equivalent MOI of MCP1 joint module. Link 1 which is fixed on the metacarpal phalange is the relative fixed frame and link 4 is chosen to be the equivalent link. The equivalent MOI as seen from the MCP1 joint is calculated in the following equation:

$$(J_{\mathrm{Ee}})_{\mathrm{MCP}}=\sum_{j=2}^{10}\left[m_j\left(\frac{{}^{1}v_{Cj}}{\dot{\alpha}_1}\right)^2+J_j\left(\frac{\omega_j}{\dot{\alpha}_1}\right)^2\right]. \tag{7}$$

Because the PIP and MCP1 joints move independently, the velocity ratio of links 5, 6 and 7 to link 4 are unknown. But we observed that some relationship might exist between movements of different joints when people move fingers. So we just take an ordinary motion, which index finger takes the flexion and extension movement in a regular speed, for example, to measure the velocity ratio aforementioned. Four healthy subjects volunteer to participate in the experiment. The subjects are asked to move their index finger freely while wearing the exoskeleton meanwhile the angular velocities of MCP1 and PIP joints are recorded by the angular sensors fixed on the exoskeleton. The results show that the angular velocities of the MCP1 and PIP joints are almost equal. The result is modeled as follows:

$$\omega_4=\omega_7 . \tag{8}$$

From Eqs. (5), (7) and (8), it is easy to know that $(J_{\mathrm{Ee}})_{\mathrm{MCP}}$ is the function of the rotating ange of link 4, that isθ_1.

Similar with other joint modules, the equivalent MOI of the actuation module can be represents as

$$(J_{\mathrm{Ea}})_{MCP}=(J_{\mathrm{D}})_{\mathrm{MCP}}+(J_{\mathrm{T}})_{\mathrm{MCP}}+(J_{\mathrm{M}}+J_{\mathrm{S}})i_{\mathrm{MCP}}^2 . \tag{9}$$

According to Eqs. (1), (5) and (7)–(9), the maximal equivalent MOI the MCP1 joint is obtained:

$$(J_{\mathrm{E}})_{\mathrm{MCPmax}}=2.17\times10^5\ \mathrm{g\cdot mm^2}.$$

The calculation shows that the exoskeleton has low moment of inertial.

4 Control System

The control system realizes both the passive and the active rehabilitation modes, of which the control requirements are different. In general, a position control algorithm is suitable for the passive mode to enable imposition of specific trajectories. A force control algroithm is needed in the active mode to control the interactive force between the device and the finger.

In this paper, we use the same controller and driver to realize the passive as well as the active rehabilitative motions based on the torque mode of the driver. In addition, the compensation of resisting torque of the system is also investigated so that human hand can move the finger easily in the active mode. The detailed control algorithm is described in the following subsections.

4.1 Active control mode

In the active motion mode, the human finger moves actively meanwhile controls the virtual hand to do the virtual exercises. Before the virtual hand contact with the virtual object (referred as to in free space) the exoskeleton follows and complies with the motion of the human finger and the human finger is supposed not to be hindered. However, the existing mechanical resistance hinders the finger's movement. A preliminary compensation method is proposed to reduce the resistance. When the virtual hand contacts with the virtual object (referred as to in constraint space) the virtual interactive force should be fed back to the human hand.

The block diagram of control structure is shown in Fig. 13.

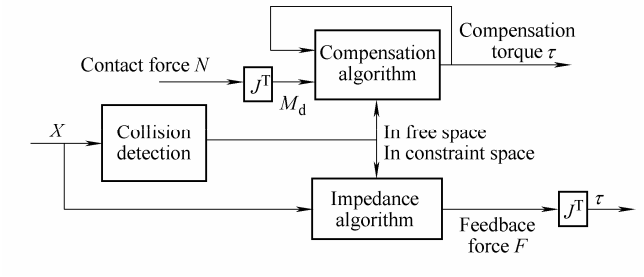

Fig. 13. Block diagram of active control mode

4.1.1 Virtual interactive force control

For the preliminary research, we confine our task to the fingertip interaction only. In the constraint space, we model the virtual interactive force as follows:

$$F = K \bullet \Delta X + B \bullet \Delta \dot{X} + M \bullet \Delta \ddot{X}, \tag{10}$$

where F is Virtual interactive force acted on the index fingertip; ΔX, $\Delta \dot{X}$, $\Delta \ddot{X}$ are vector of penetration depth, velocity and acceleration of the fingertip, respectively; M, B, K are inertial properties, damping and stiffness coefficients, respectively.

We calculate the feedback torques τ on DIP, PIP and MCP joints according to the equilibrium equation of moment to try to approximate the realistic feelings:

$$\tau = J^{\mathrm{T}} \bullet F, \tag{11}$$

where J is the Jacobian matrix which is determined bu the grasp configuration.

4.1.2 Resistance compensation control in free space

When the patient moves the finger actively in free space while wearing the device, the resistance in the system hinders the movement of the finger, increases the difficulty for patients to accomplish the rehabilitation exercises, and reduces the realism in virtual rehabilitation. We proposed a method to compensate the resistance. For the continuous motion of abduction/adduction, the resistance of our device is not obvious. We only focus on the resistance compensation for the flexion and extension in the subsequent part. We simplify the mechanical models for one finger joint as shown in Fig. 14.

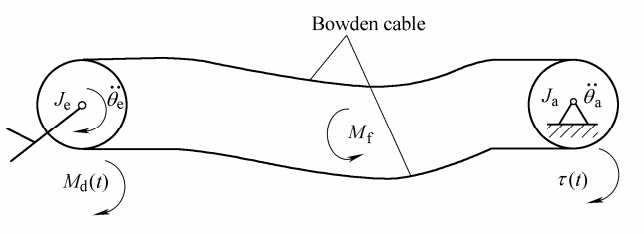

Fig. 14. Simplified model for one finger joint

Considering that the patient hand has limited motor capability and the hand usually moves slowly, so in the mechanical model the effect of velocity is ignored. According to the equilibrium equation of the moment, at a certain time t, we have

$$M_{\mathrm{d}}(t) + \tau(t) = J_{\mathrm{e}} \bullet \ddot{\theta}_{\mathrm{e}}(t) + J_{\mathrm{a}} \bullet \ddot{\theta}_{\mathrm{a}}(t) + M_{\mathrm{f}}(t), \tag{12}$$

where $M_{\mathrm{d}}(t)$ —Driving torque which is produced by the fingertip-exerted force;

$\tau(t)$ —Output torque of the actuator module which is used to compensate the system resistance;

$M_{\mathrm{f}}(t)$ —Resistance torque generated by the mechanical friction;

J_{e}, J_{a} —Moment of inertia of the exoskeleton module and of the actuator module, respectively;

$\ddot{\theta}_e(t)$, $\ddot{\theta}_a(t)$ —Corresponding angular acceleration, respectively.

If we want to compensate the mechanical resistance caused by the friction and the moment of inertia, the actuator module output $\tau(t)$ should be

$$\tau(t) = J_{\mathrm{e}} \bullet \ddot{\theta}_{\mathrm{e}}(t) + J_a \bullet \ddot{\theta}_{\mathrm{a}}(t) + M_{\mathrm{f}}(t). \tag{13}$$

Because $M_{\mathrm{f}}(t)$ at time t is unknown, so we estimate $\tau(t)$ with the total input torque at time $t-1$. Considering that the time interval is small so the estimation is reasonable. So we have

$$\tau(t) = M_{\mathrm{d}}(t-1) + \tau(t-1). \tag{14}$$

The active rehabilitative motion requires that it is the human hand that drives the exoskeleton. However, if the estimated $\tau(t)$ is greater than the actual resistance torque, the exoskeleton is then driven by the actuator, and the active rehabilitative motion is switched to passive rehabilitative motion which is not desired. On the other hand, the human fingertip will not contact with the sensors which means the contact force cannot be measured. Therefore we modify equation (14) as follows:

$$\tau(t) = \xi \bullet [M_{\mathrm{d}}(t-1) + \tau(t-1)] \quad (\xi \leqslant 1.0). \tag{15}$$

The coefficient ξ is determined by experiment. The driving torque $M_{\mathrm{d}}(t-1)$ could be calculated from the jacobian matrix given that the contact force N measured from the force sensors.

Since the DIP, PIP, and MCP1 joints have the similar structure and are controlled independently, the proposed method can be used for every joint.

However, the method can only be realized during the motion of flexion, since for the motion of extension, the contact force cannot be measured yet.

4.2 Passive mode control

In the passive control mode, the control objective is to drive the joints to the desired positions. Thus, the position control is carried out.

We use the PID controller here. The block diagram of passive control mode is shown in Fig. 15.

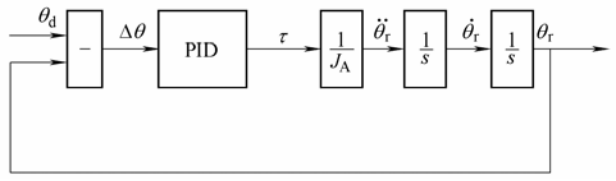

Fig. 15. Block diagram of passive control mode

The position error $\Delta\theta$ is used to control the output torque of the motor τ. $\Delta\theta$ and τ are determined as follows:

$$\Delta\theta = \theta_r - \theta_d, \tag{16}$$

$$\tau = K_P \bullet \Delta\theta + K_I \bullet \int \Delta\theta \bullet dt + K_D \bullet \frac{d\Delta\theta}{dt}, \tag{17}$$

where θ_d —Desired angle of exoskeleton;
θ_r —Actual angle of finger joint read from the potentiometer;
$\Delta\theta$ —Position difference between θ_d and θ_r;
τ —Output torque of the motor;
K_P —Proportional coefficient;
K_I —Integral coefficient;
K_D —Differential coefficient.

4.3 Experimental Result

In this experiment, the subject's hand wears the exoskeleton and moves the index finger to control the virtual finger to touch the virtual box. The subject is supposed to feel unhindered in the free space and feel the force feedback in the constraint space. During the experiments, the force is measured by the force sensors on the fingertip. The accuracy of the force sensor is 10 mN.

4.3.1 Resistance compensation

In the free space, the control is implemented with and without the resistance compensation, respectively, and the corresponding force output by the human fingertip is shown in Fig. 16 for comparison. With the resistance compensation, the coefficient ξ in Eq. (14) is set as ξ=0.9.

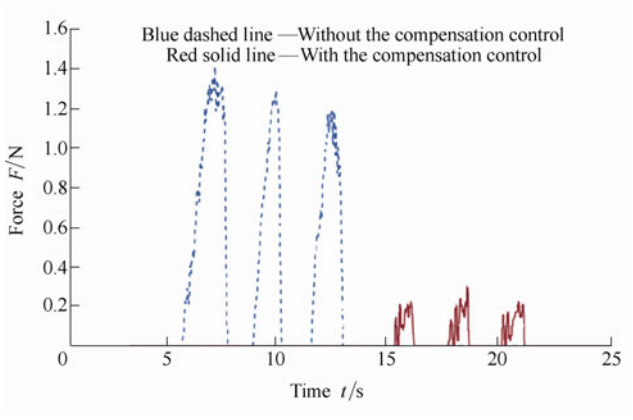

Fig. 16. Force exerted by fingertip

Based on the experimental result, with the compensation control algorithm, the maximum output force of the human fingertip is less than one third of the maximum force without compensation during the motion of flexion.

4.3.2 Virtual interactive force

Fig. 17 shows that the feedback force applied on the fingertip in constraint space. The parameters determined by experiments are K=0.5 N/mm, B=M=0.

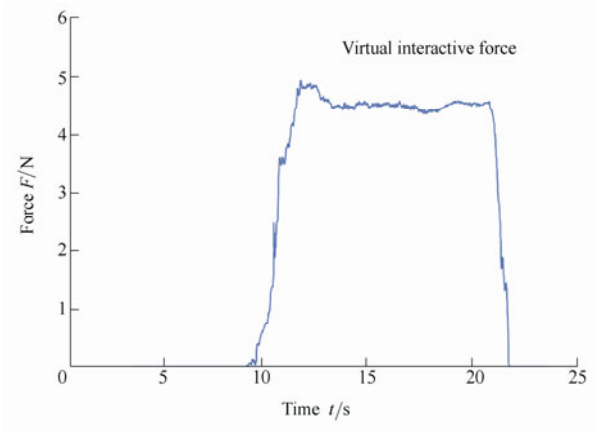

Fig. 17. Virtual interactive force

From the time 0 to 6, the virtual finger doesn't contact with the virtual box. At the 6, the virtual hand begins to contact with the virtual box, and the virtual interactive force is generated and fed back to the human finger. The contact lasts about 9, and at the time 15 the virtual finger departs from the virtual box. Fig. 17 shows that the virtual interactive force is implemented successfully.

4.3.3 Passive motion control

The target is to control the exoskeleton joint to rotate along a predefined trajectory, here a sinusoidal path with the amplitude of 0.5π radian, and the period of 10 seconds. The experimental results are shown in Fig. 18, Fig. 19 and Fig. 20.

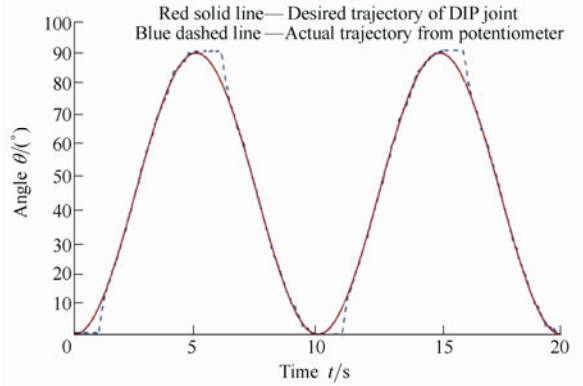

Fig. 18. DIP joint trajectories
(K_P = 63.24 m Nm/rad, K_I = 1.26 m Nm/rad, K_D = 77.15 m Nm/rad)

The exoskeleton could follow the predefined trajectory at most of the time except when flexion change to extension

or vice versa. At the transition moment, the device must overcome the great static friction. While the driving force is determined by the position difference between the desired angle and the actual angle of the exoskeleton. So when the driving force is less than the friction, the exoskeleton doesn't move. This suggests further investigation to obtain the better results.

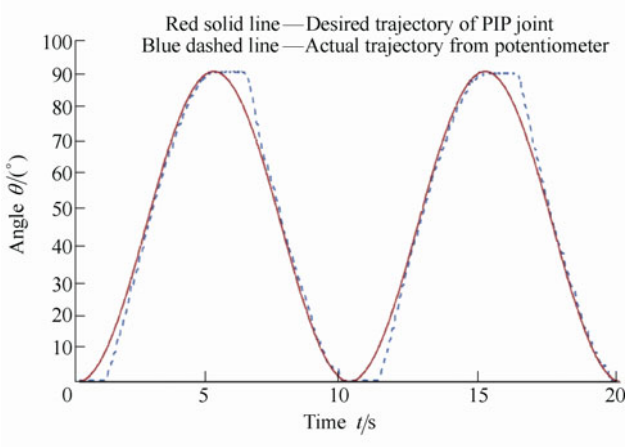

Fig. 19. PIP joint trajectories
($K_P = 69.26$ m Nm/rad, $K_I = 1.39$ m Nm/rad, $K_D = 84.5$ m Nm/rad)

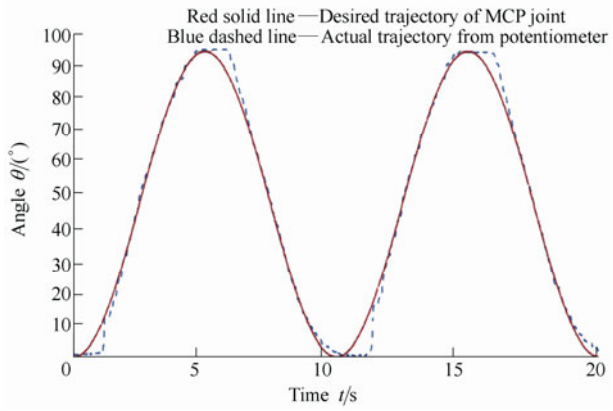

Fig. 20. MCP joint trajectories
($K_P = 79.05$ m Nm/rad, $K_I = 1.581$ m Nm/rad, $K_D = 96.44$ m Nm/rad)

5 Conclusions

(1) An hand exoskeleton system for index finger rehabilitation is introduced which can simultaneously accomplish the active and passive rehabilitation.

(2) The special characteristics of the proposed device includes lightweight, low inertial, able to independently control all finger joints, accommodation to different hand sizes, changeable ROM and mechanical safety design.

(3) The proposed control strategy can realize position control and force control with the motor driver which only works in force control mode. Besides, the mechanical resistance is effectively compensated.

(4) With sets of experiments, the above mentioned characteristics are verified and the feasibility of the system is proven.

(5) The experiments show that the friction between the cables and sheaths greatly affects the performances of the device. So the friction compensation will be researched in further.

References

[1] TAO Quan. *Hand rehabilitation* [M]. Shanghai: Shanghai Jiao Tong University Press, 2006. (in Chinese)

[2] KERBS H I, VOLPE B T, AISEN M L, et al. Increasing productivity and quality of care: Robot-aided neuro-rehabilitation[J]. *Journal of Rehabilitation Research and Development*, 2000, 37(6): 639–652.

[3] FISCHER H C, STUBBLEFIELD K, Kline T, et al. Hand rehabilitation following stroke: A pilot study of assisted finger extension training in a virtual environment[J]. *Topics in Stroke Rehabilitation*, 2007, 14(1): 1–12.

[4] LU Guangming, SUN Lining, PENG Longgang. Analysis of the status and the key technology of the robot technology for rehabilitation[J]. *Journal of Harbin Institute of Technology*, 2004, 36(9): 1 224–1 231.

[5] LAMBERCY O, DOVAT L, GASSERT R, et al. A haptic knob for rehabilitation of hand function[J]. *IEEE Transaction on Neural Systems and Rehabilitaiton Engineering*, 2007, 15(3): 356–366.

[6] MALI U, MUNIH M. HIFE-Haptic interface for finger exercise[J]. *IEEE/ASME Transactions on Mechatronics*, 2006, 11(1): 93–102.

[7] DOVAT L, LAMBERCY O, JOHNSON V, et al. A cable driven robotic system to train finger function after stroke[C]// *Proceedings of the 2007 IEEE 10th International Conference on Rehabilitation Robotics*, Noordwijk, Netherlands, June 13–15, 2007: 222–227.

[8] IMMERSION. CyberGrasp™ User's Guide [EB/OL]. 2009-12-07 [2001-04-20]. http://www.cyberglovesystems.com/products/cybergrasp/overview

[9] BOUZIT M, BURDEA G, POPESCU G, et al. The Rutgers Master II —New design force–feedback glove[J]. *IEEE/ASME Transactions on Mechatronics,* 2002, 7(2): 256–263.

[10] LELIEVELD M J, MAENO T, TOMIYAMA T. Design and development of two concepts for a 4 DOF portable haptic interface with active and passive multi-point force feedback for the index finger[C]// *ASME International Design Engineering Technical Conference & Computers and Information in Engineering Conference*, Philadelphia, Pennsylvania, USA, September 10–13, 2006: 1–10.

[11] ITO S, KAWASAKI H, ISHIGRE Y. A design of fin motion assist equipment for disabled hand in robotic rehabilitation system[J]. *Journal of the Franklin Institute,* 2011, 348 (1): 79–89.

[12] FU Yili, WANG Peng, WANG Shuguo, et al. Design and development of a portable exoskeleton based CPM machine for rehabilitation of hand injuries[C]// *IEEE International Conference on Robotics and Biomimetics,* Sanya, China, December 15–18, 2007: 1 476–1 481.

[13] WEGE A, KONDAK K, HOMMEL G. Mechanical design and motion control of a hand exoskeleton for rehabilitation[C]// *IEEE International Conference on Mechatronics and Automation*, Niagara Falls, Ontario, Canada, July 29–August 1, 2005: 155–159.

[14] WORSNOPP T T, PESHKIN M A, COLGATE J E, et al. An actuated finger exoskeleton for hand rehabilitation following stroke[C]//*IEEE 10th International Conference on Rehabilitation Robotics*, Noordwijk aan Zee, Netherlands, June 13–15, 2007: 896–901.

[15] YAMAURA H, MATSUSHITA K, KATO R, et al. Development of hand rehabilitation system for paralysis patient—Universal design using wire-driven mechanism[C]//*31th Annual International*

conference of the IEEE-EMBS, MN, USA, September 2–6, 2009: 7 122–7 125.

[16] CHIRI A, GIOVACCHINI F, VITIELLO N, et al, HANDEXOS: towards an exoskeleton device for the rehabilitation of the hand[C]// *The 2009 IEEE/RSJ International Conf. on Intelligent Robots and Systems*, St. Louis, USA, October 11–15, 2009: 1 106–1 111.

[17] BUCHHOLZ B, ARMSTRONG T, GLODSTEIN S. Anthropometric data for describing the kinematics of the human hand[J]. *Ergonomics*,1992, 35(3): 261–273.

[18] MOURI T, KAWASAKI H, NISHIMOTO Y, et al. Development of robot hand for therapist education/training on rehabilitation[C]// *Proceedings of the 2007 IEEE/RSJ International Conference on Intelligent Robots and Systems*, San Diego, CA, USA, Oct. 29–Nov.2, 2007: 2 295–2 300.

[19] WANG Ju, LI Jiting, ZHANG Yuru, et al. Design of an exoskeleton for index finger rehabilitation[C]// *Proceedings of the 31th Annual International Conference of the IEEE EMBS*, Minneapolis, MN, USA, September 2-6, 2009: 5 957–5 960.

[20] JIANG Li, CUTKOSKY M R, RUUTIAINEN J, et al. Using haptic feedback to improve grasp force control in multiple sclerosis patients[J]. *IEEE Transaction on Robotics*, 2009, 25(3): 593–601.

[21] ZHANG Yuru, LI Jiting, LI Jianfeng. *Robot dexterous hand: Modeling, Planning and Simulation*[M]. Beijing: China Machine Press, 2007.

Biographical notes

LI Jiting, born in 1967, is currently an associate professor at *State Key Laboratory of Virtual Reality Technology and Systems, Robotics Institute, Beihang University, China.* Her research interests include robot kinematics and dynamics, haptic interfaces, and virtual rehabilitation.
Tel: +86-10-82317750; E-mail: lijiting@buaa.edu.cn

WANG Shuang, born in 1985, is currently a master candidate at *State Key Laboratory of Virtual Reality Technology and Systems, Robotics Institute, Beihang University, China.*
E-mail: wangshuang_110@yahoo.com.cn

WANG Ju, born in 1985, is currently a master candidate at State *Key Laboratory of Virtual Reality Technology and Systems, Robotics Institute, Beihang University, China.*
E-mail: wangju1985@gmail.com

ZHENG Ruoyin, born in 1986, is currently a master candidate at *State Key Laboratory of Virtual Reality Technology and Systems, Robotics Institute, Beihang University, China.*
E-mail: ryzheng860909@126.com

ZHANG Yuru, born in 1959, is currently a professor at *State Key Laboratory of Virtual Reality Technology and Systems, Robotics Institute, Beihang University, China*. Her research is focused on the design of new mechanisms for a variety of applications including robotics, haptic interface, rehabilitation, tele-operation and virtual prototyping.
Tel: +86-10-82338023; E-mail: yuru@buaa.edu.cn

CHEN Zhongyuan, born in 1987, is currently a master candidate at *State Key Laboratory of Virtual Reality Technology and Systems, Robotics Institute, Beihang University, China.*
E-mail: czy159157@163.com;